Autonomous Vehicle Positioning With GPS in Urban Canyon Environments

Youjing Cui and Shuzhi Sam Ge, *Senior Member, IEEE*

***Abstract*—The Global Positioning System (GPS) has been widely used in land vehicle navigation applications. However, the positioning systems based on GPS alone face great problems in the so-called urban canyon environments, where the GPS signals are often blocked by highrise buildings and there are not enough available satellite signals to estimate the positioning information of a fix. To solve the problem, a constrained method is presented by approximately modeling the path of the vehicle in the urban canyon environments as pieces of lines. By adding this constraint, the minimum number of available satellites reduces to two, which is satisfied in many urban canyon environments. Then, different approaches using the constrained method are systematically developed. In addition, a state-augmentation method is proposed to simultaneously estimate the positions of the GPS receiver and the parameters of the line. Furthermore, the interacting multiple model method is used to determine the correct path which the vehicle follows after passing an intersection of roads. Simulation results show that this approach can solve the urban canyon problems successfully.**

***Index Terms*—Extended Kalman filtering, Global Positioning System (GPS), interacting multiple model, joint parameter and state estimation.**

I. Introduction

THE GLOBAL Positioning System (GPS) has been widely used as a component in land vehicle navigation systems. However, the positioning systems based on GPS are challenged by urban canyon environments in terms of delivery of enough continuous positioning information. To obtain the positioning information of a fix, signals from at least four satellites are required. However, in urban areas, GPS signals are often blocked by highrise buildings (in the so-called "urban canyons"). This means that for a significant percentage of the journey time, a pointwise position solution is not available.

To tackle the problem associated with GPS in urban canyon environments, several approaches have been proposed as detailed below.

1) To increase the number of visible satellites. In [3], [9], the Russian Global Navigation Satellite System (GLONASS) is used to augment the GPS by offering more satellites in view and thus, increasing the satellites' availability. Advanced GPS receivers [10], [11] have been developed which can access up to eight or more GPS satellites, and to thereby minimize any risk of urban blockage.

2) To find a constrained solution. For example, in marine vehicle applications, the altitude could be defined as sea level [1]. In land vehicle applications, if the altitude changes slowly, it is often considered constant and assumed to be known [7].

3) To use external references [1] such as an altimeter or a precise clock [8].

4) To integrate the GPS with dead reckoning sensors such as intertial navigation systems (INS) and encoders to provide continuous positioning information [2]–[6].

5) To solve the urban canyon problem by modeling the dynamics and using a Kalman-filter-based approach. The Kalman filtering method has been widely used in robot self-localization [23], [24] as well as GPS applications [25]–[27]. The Kalman filter time update always provides a position estimate, even if no pseudorange measurements are available. But the covariance of this estimate will increase in at least one direction when the number of independent range measurements is less than four [1].

In this paper, another constrained solution is proposed to solve the problem by approximately modeling the path of the vehicle as pieces of curves such as straight lines, arcs, polynomials, and so on. As the vehicle travels in an urban area, its path is always constrained in a certain piece of road. By approximately modeling the path of the vehicle as a line resembling the road known *a priori*, fewer GPS satellites are necessary to obtain the positioning information. In fact, the minimum number of the available satellites drops to two. Fortunately, detailed maps are usually available for most cities. Accordingly, the city map can be modeled as junctions connected by piecewise continuous lines. In such a manner, the information of the map is stored in the database of the proposed GPS positioning system.

Though an approximate model of the vehicle's path can be obtained from the map database, the actual path may deviate from the approximate model and is to be estimated. In this paper, the state augmentation method and the extended Kalman filtering (EKF) technique are used together to simultaneously estimate the parameters of the actual path and the positioning information.

To enable the vehicle to be capable of choosing the right road model after passing an intersection, some probabilistic approach needs to be adopted to solve the multiple hypotheses problem. Many statistical techniques, such as the nearest neighbor algorithm [13], the track-splitting filter [13], the joint-likelihood algorithms [13], and the Markov approaches [14]–[16], have been used for data association and robot navigation applications. In

Manuscript received August 27, 2001. This paper was recommended for publication by Associate Editor D. Pai and Editor S. Hutchinson upon evaluation of the reviewers' comments. This paper was presented in part at the IEEE International Conference on Robotics and Automation, Seoul, Korea, May 21-26, 2001.

The authors are with the Department of Electrical and Computer Engineering, National University of Singapore, Singapore 117576 (e-mail: elegesz@nus.edu.sg).

Digital Object Identifier 10.1109/TRA.2002.807557

this paper, the interacting multiple model (IMM) algorithm is employed to solve the multiple hypotheses problem. The IMM method has been widely used in multitarget tracking applications [18], [19], [21]. It is also used to improve the signal-to-noise ratio (SNR) for noisy speech [17]. In this paper, the IMM method combined with EKF is used to estimate the position of a vehicle at intersection areas and to choose the correct road from all the roads connected to this intersection as it leaves the intersection.

The paper is organized as follows. Section II briefly describes the urban canyon problem associated with GPS and presents the concept of the new constrained solution to it. Section III develops pointwise and filtering approaches to implementing the constrained solution. In Section IV, a general method by combining the state augmentation technique and the EKF method is presented to estimate the parameters of the curve model of the vehicle's path and the positioning information simultaneously. Section V focuses on solving the multiple hypotheses problem encountered when the vehicle meets an intersection by the IMM method. In Section VI, the performance of the proposed approach is analyzed. In Section VII, simulation studies reveal the feasibility and effectiveness of the proposed approach.

II. Problem Formulation

GPS positioning is often solved in the earth-fixed rectangular coordinate system, where the user's position is denoted by (x, y, z) and the ith satellite position is denoted by (X_i, Y_i, Z_i) and $i = 1, 2, \ldots, n_j$, with n_j being the number of the available satellites. The pseudorange measurement, ρ_i, from the ith satellite to the user is given by

$$\rho_i = \rho_{i0} + B_r + v_i, \qquad i = 1, 2, \ldots, n_j \tag{1}$$

where $\rho_{i0} = \sqrt{(X_i - x)^2 + (Y_i - y)^2 + (Z_i - z)^2}$ is the actual range from the ith satellite to the user, B_r is the distance corresponding to the user's clock bias with respect to the GPS time, and v_i represents all the other errors contributed to the pseudorange measurements. If stand-alone GPS is used, v_i's contain some common mode errors, and thus, are correlated to each other. If differential GPS (DGPS) is adopted, the common mode errors in v_i are eliminated through differencing. Thus, v_i contains only uncommon mode errors and can be considered as uncorrelated to each other. In this case, the error terms can be approximately characterized by zero-mean Gaussian white noise with a typical standard deviation of 1 m. Since the satellite positions can be precomputed from the ephemeris data, the user position and clock bias can be derived from (1) by neglecting v_i. Since there are four unknowns, x, y, z, and B_r, in the pseudorange equations, at least four satellites are needed at each epoch.

When a vehicle with a GPS receiver on board travels in urban areas, the GPS signals are often blocked by highrise buildings which form the so-called urban canyon environments. In such situations, if the number of available satellites is less than four at a given epoch, then the complete GPS solution cannot be obtained through the pseudorange equations (1) directly.

As mentioned in Section I, several approaches have been proposed to tackle the problem associated with GPS in urban canyon environments. In this paper, another constrained solution is provided to solve the problem by approximately modeling the path of the vehicle by pieces of curves in the urban canyon environments. As the vehicle travels in an urban area, its path is always confined in a certain piece of road. By modeling the path of the vehicle as a curve resembling the shape of the road, fewer GPS satellites are necessary to obtain the positioning information.

Generally, a curve in space can be regarded as the intersection of two surfaces. Recall that any surface in space can be described by $S(x, y, z) = 0$. Therefore, a curve can be generally modeled by

$$\begin{cases} S_1(x, y, z) = 0 \\ S_2(x, y, z) = 0. \end{cases} \tag{2}$$

Combining (1) and the two equations in the general line model (2) leads to $n_j + 2$ equations at each epoch with four unknowns, the current position (x, y, z) and the user's clock bias B_r, provided that the parameters of the line are known *a priori*. To obtain the four unknowns at each epoch, the number of equations cannot be less than four, i.e., $n_j \geq 2$. Thus, the minimum number of satellites to obtain the position and clock bias information drops to two.

The operations of the overall GPS-based positioning system are as follows. When the GPS receiver is able to access enough satellite signals with good geometry, the positioning information will be estimated through a traditional approach by using the pseudorange equation (1) only. If the vehicle travels in urban canyon environments, some GPS signals are lost by blockage. In this case, the positioning system estimates the positioning information by utilizing both the available GPS signals (suppose that there are at least two GPS satellites in view) and the model of the path of the vehicle. If the urban canyon environment is a road intersection, then the IMM method is used to estimate the position of the vehicle and determine the correct path model which the vehicle follows.

III. Solutions

If the curve model of the path of the vehicle is known, the positioning information of the vehicle can be calculated from two (or more) pseudorange equations and the curve model. Notice that in reality, most pieces of roads are straight lines, arcs, or other simple smooth curves. Therefore, without losing generality, assume that both y and z can be written as an explicit function of x. Then, a road can be simply modeled by

$$\begin{cases} y = f_1(x) \\ z = f_2(x). \end{cases} \tag{3}$$

Thus, for the case of m available satellites, where $m \geq 2$, the set of equations to be solved are

$$\rho_i = \rho_{i0} + B_r + v_i, \qquad i = 1, \ldots, m \tag{4}$$

$$y = f_1(x) \tag{5}$$

$$z = f_2(x). \tag{6}$$

Basically, the solutions to this problem fall into two categories, the pointwise solution, which estimates the current positioning information using only the current available information, and the filtering solution, which utilizes both the current information and previous information to give the current positioning estimates. For the point solutions, there exist two kinds

of approaches: 1) the direct approach, which solves the nonlinear equations directly and obtains a closed-form solution; and 2) the indirect approach, which is based on linearization of the measurement equations. For $m > 2$, usually no solution can be obtained due to the measurement noises by using the direct solution. Even for the case of $m = 2$, since (5) and (6) are generally also nonlinear and it is difficult to solve (4)–(6) directly. Therefore, only the indirect approach and the Kalman filtering approach are discussed in this section.

A. Indirect Solution

Substituting (5) and (6) into (4) and linearizing the resulting equations about $x = x_0$ leads to

$$\boldsymbol{\rho}(x) = \boldsymbol{\rho}_0(x_0) + \mathbf{H}\delta\mathbf{x} + \mathbf{v} + \mathcal{O}(\delta x) \tag{7}$$

where

$$\begin{aligned}
\boldsymbol{\rho}(x) &= [\rho_1(x), \ldots, \rho_m(x)]^T \\
\boldsymbol{\rho}_0(x_0) &= [\rho_{10}(x_0), \ldots, \rho_{m0}(x_0)]^T \\
\delta\mathbf{x} &= [\delta x,\ B_r]^T, \quad \mathbf{v} = [v_1, \ldots, v_m]^T \\
\rho_{i0}(x) &= \sqrt{(X_i - x)^2 + (Y_i - f_1(x))^2 + (Z_i - f_2(x))^2}
\end{aligned}$$

and

$$\mathbf{H} = \left.\begin{bmatrix} H_1 & 1 \\ \vdots & \vdots \\ H_m & 1 \end{bmatrix}\right|_{x=x_0}$$

with

$$H_i = \frac{\partial \rho_i}{\partial x} = \frac{1}{\rho_{i0}(x)}[x - X_i + (f_1(x) - Y_i)f_1'(x) + (f_2(x) - Z_i)f_2'(x)] \tag{8}$$

where $i = 1, \ldots, m$. Since the number of measurement equations is greater than or equal to the number of unknowns, the least-squares method is adopted, and the solution is given by

$$\delta\hat{\mathbf{x}} = (\mathbf{H}^T\mathbf{H})^{-1}\mathbf{H}^T\delta\boldsymbol{\rho} \tag{9}$$

by assuming that $(\mathbf{H}^T\mathbf{H})$ is nonsingular, where $\delta\boldsymbol{\rho} = \boldsymbol{\rho} - \hat{\boldsymbol{\rho}}_0$.

With knowledge of the position error $\delta\hat{x}$, the actual position is determined as

$$\hat{\mathbf{p}} = \mathbf{p}_0 + \begin{bmatrix} \delta\hat{x} \\ \delta\hat{y} \\ \delta\hat{z} \end{bmatrix} = \mathbf{p}_0 + \begin{bmatrix} \delta\hat{x} \\ \delta\hat{x}f_1'(x_0) \\ \delta\hat{x}f_2'(x_0) \end{bmatrix}. \tag{10}$$

B. Kalman Filtering Solution

Kalman filtering has been the standard method used in most GPS receivers to provide user position and velocity outputs [1]. By noting that the pseudorange equation (1) is inherently nonlinear, the EKF technique is adopted herein to estimate the positioning information.

Assumption 1: Assume that DGPS is used in the positioning system instead of stand-alone GPS.

Under this assumption, the noises v_i in the pseudorange measurements can be regarded as uncorrelated to each other, and the error terms can be approximately characterized by zero-mean Gaussian white noises, which facilitates the system modeling for Kalman filtering. If stand-alone GPS is adopted, v_i contains some common mode errors, and thus, are correlated to each other. Therefore, the Kalman filtering method cannot be applied directly. Of course, one can still use the Kalman filtering approach in this case by properly modeling the common mode errors. For simplicity of presentation, only the DGPS case is studied in this paper. In order to understand the EKF approach for position estimation in the case of urban canyon environments more clearly, first, the EKF solution for the case where there are enough GPS satellites is discussed.

1) In Non-Urban-Canyon Area: When the receiver is in low dynamic motion, (i.e., near constant velocity), the velocity is modeled as a random-walk process, and the position is modeled as the integral of velocity. Physically, the clock bias develops as the integral of the frequency error of the receiver clock oscillator [1]. Thus, the receiver clock bias can be described by a two-state model

$$\begin{bmatrix} \dot{B}_r(t) \\ \ddot{B}_r(t) \end{bmatrix} = \begin{bmatrix} 0 & 1 \\ 0 & 0 \end{bmatrix}\begin{bmatrix} B_r(t) \\ \dot{B}_r(t) \end{bmatrix} + \begin{bmatrix} w_\phi(t) \\ w_f(t) \end{bmatrix} \tag{11}$$

where w_ϕ and w_f are the process noises driving the phase and the frequency error states, respectively. Then, the state-space model for the GPS receiver is given by

$$\mathbf{x} = \mathbf{F}\mathbf{x} + \mathbf{w} \tag{12}$$

where

$$\begin{aligned}
\mathbf{x} &= [x \quad y \quad z \quad B_r \quad \dot{x} \quad \dot{y} \quad \dot{z} \quad \dot{B}_r]^T \\
\mathbf{F} &= \begin{bmatrix} \mathbf{0}_{4\times4} & \mathbf{I}_{4\times4} \\ \mathbf{0}_{4\times4} & \mathbf{0}_{4\times4} \end{bmatrix} \\
\mathbf{w} &= [0 \quad 0 \quad 0 \quad w_{B_r} \quad w_{vx} \quad w_{vy} \quad w_{vz} \quad w_{dB_r}]^T
\end{aligned}$$

The w_v terms would be selected to model the random variations in the velocity. Obviously, this state-space model is linear. The pseudorange equation (1) is regarded as the measurement equation, which can be rewritten as

$$\boldsymbol{\rho} = \mathbf{h}(\mathbf{x}) + \mathbf{v} \tag{13}$$

where

$$\boldsymbol{\rho} \in R^m, \qquad \mathbf{h}(\mathbf{x}) = [\rho_{i0} + B_r] \in R^m, \quad \text{and} \quad \mathbf{v} \in R^m.$$

Equations (12) and (13) are a continuous-time model for the system. The corresponding discrete-time model is described by

$$\mathbf{x}(k+1) = \boldsymbol{\Phi}\mathbf{x}(k) + \mathbf{w}_d(k) \tag{14}$$

$$\boldsymbol{\rho}(k) = \mathbf{h}[\mathbf{x}(k)] + \mathbf{v}(k) \tag{15}$$

where $\boldsymbol{\Phi} = e^{\mathbf{F}T_s}$ with T_s being the sampling period, and $\mathbf{w}_d(k)$ is a discrete-time white Gaussian sequence that is statistically equivalent through its first two moments to $\int_{t_k}^{t_{k+1}} \boldsymbol{\Phi}\mathbf{w}(\tau)\,d\tau$ [12].

Under the assumption that the noises, $\mathbf{w}_d$ and $\mathbf{v}$, are zero-mean normal distributed white noises and are characterized by covariance matrices, $\mathbf{Q}_d$ and $\mathbf{R}$, respectively, the EKF equations are given by

$$\hat{\mathbf{x}}^-(k) = \boldsymbol{\Phi}\hat{\mathbf{x}}^+(k-1) \tag{16}$$

$$\mathbf{P}^-(k) = \boldsymbol{\Phi}\mathbf{P}^+(k-1)\boldsymbol{\Phi}^T + \mathbf{Q}_d \tag{17}$$

$$\mathbf{K}(k) = \mathbf{P}^-(k)\mathbf{H}^T(k)\left[\mathbf{H}(k)\mathbf{P}^-(k)\mathbf{H}^T(k) + \mathbf{R}(k)\right]^{-1} \tag{18}$$

$$\mathbf{P}^+ = [\mathbf{I} - \mathbf{K}(k)\mathbf{H}(k)]\mathbf{P}^-(k) \tag{19}$$

$$\hat{\mathbf{x}}^+(k) = \hat{\mathbf{x}}^-(k) + \mathbf{K}(k)[\boldsymbol{\rho}(k) - \mathbf{h}(\mathbf{x}^-(k))] \tag{20}$$

where

$$\mathbf{H}(k) = \left.\frac{\partial \mathbf{h}(\mathbf{x})}{\partial \mathbf{x}}\right|_{\mathbf{x}=\mathbf{x}^-(k)} = \left.[[H_{ij}]_{m\times4} \quad \mathbf{0}_{m\times4}]\right|_{\mathbf{x}=\mathbf{x}^-(k)}$$

with

$$H_{i1}=\frac{\partial\rho_i}{\partial x}=\frac{1}{\rho_{i0}}(x-X_i),\quad H_{i2}=\frac{\partial\rho_i}{\partial y}=\frac{1}{\rho_{i0}}(y-Y_i),$$
$$H_{i3}=\frac{\partial\rho_i}{\partial z}=\frac{1}{\rho_{i0}}(z-Z_i),\quad H_{i4}=1.$$

2) In Urban Canyon Environment: In the urban canyon environment, we shall use (4)–(6) to estimate the positioning information. Since y and z are functions of x according to (5) and (6), the states chosen to describe the dynamics of the receiver become

$$\mathbf{x}_1=[x\quad B_r\quad \dot{x}\quad \dot{B}_r]^T. \tag{21}$$

The state-space model is given by

$$\dot{\mathbf{x}}_1=\mathbf{F}_1\mathbf{x}_1+\mathbf{w}_1 \tag{22}$$

where

$$\mathbf{F}_1=\begin{bmatrix}\mathbf{0}_{2\times2} & \mathbf{I}_{2\times2}\\ \mathbf{0}_{2\times2} & \mathbf{0}_{2\times2}\end{bmatrix}$$
$$\mathbf{w}_1=[0\quad w_{B_r}\quad w_{vx}\quad w_{dB_r}]^T.$$

The measurement equation is also given by (1) which can also be written in the following form

$$\boldsymbol{\rho}(t)=\mathbf{h}_1(\mathbf{x}_1(t))+\mathbf{v}(t) \tag{23}$$

where $\mathbf{h}_1(\mathbf{x}1)=[h_{1i}]\in R^m$ with $h_{1i}=\rho_{i0}+B_r$.

The EKF solution to (22) and (23) is similar to (14)–(20). Note that the matrix $\mathbf{H}$ in (18) and (19) becomes

$$\mathbf{H}_1(k)=\left.\frac{\partial\mathbf{h}_1(\mathbf{x}_1)}{\partial\mathbf{x}_1}\right|_{\mathbf{x}_1=\mathbf{x}_1^-(k)}=[H_{1ij}]\big|_{\mathbf{x}_1=\mathbf{x}_1^-(k)}\in R^{m\times4}$$

with

$$\mathbf{H}_{1i1}=\frac{1}{\rho_{i0}}[x-X_i+(f_1(x)-Y_i)f_1'(x)+(f_2(x)-Z_i)f_2'(x)]$$
$$\mathbf{H}_{1i2}=1,\quad \mathbf{H}_{1i3}=0,\quad \mathbf{H}_{1i4}=0.$$

IV. State-Augmented EKF

In Section III, solutions to (4)–(6) are studied by assuming that both the type and the parameters of the curve model of the vehicle's path are known *a priori*. In real implementation, though the mathematical model for a certain road can be achieved from the map, the actual path of the vehicle may deviate from this model. Therefore, in real implementations, a model for the path of the vehicle is established which resembles the form of the road model, but whose parameters are unknown and to be estimated. In this paper, the state augmentation method and the EKF technique are used together to estimate the parameters of the line and the positioning information simultaneously.

The fundamental concept of state augmentation is to treat the unknown parameters of the curve also as states. The curve of the vehicle's path with unknown parameters can be written as

$$\begin{cases}y=f_1(x,\mathbf{p}_c)\\ z=f_2(x,\mathbf{p}_c)\end{cases} \tag{24}$$

where $\mathbf{p}_c=[p_1,p_2,\ldots,p_l]^T$ denotes the unknown parameters of the curve and l is the number of the parameters to be estimated.

The resulting state-space model is given by

$$\dot{\mathbf{x}}_2=\mathbf{F}_2\mathbf{x}_2+\mathbf{w}_2 \tag{25}$$

where

$$\mathbf{x}_2=[x\quad B_r\quad \dot{x}\quad \dot{B}_r\quad p_1\quad p_2\quad\cdots\quad p_l]^T\in R^{4+l}$$
$$\mathbf{F}_2=\begin{bmatrix}\mathbf{F}_{21} & \mathbf{0}_{4\times l}\\ \mathbf{0}_{l\times4} & \mathbf{0}_{l\times l}\end{bmatrix}\in R^{(4+l)\times(4+l)}$$
$$\mathbf{w}_2=[0\quad w_{B_r}\quad w_{vx}\quad w_{dB_r}\quad \mathbf{0}_{1\times l}]^T\in R^{4+l}$$

with

$$\mathbf{F}_{21}=\begin{bmatrix}\mathbf{0}_{2\times2} & \mathbf{I}_{2\times2}\\ \mathbf{0}_{2\times2} & \mathbf{0}_{2\times2}\end{bmatrix}.$$

According to (1), the measurement equation can be written as

$$\boldsymbol{\rho}(t)=\mathbf{h}_2(\mathbf{x}_2(t))+\mathbf{v}(t) \tag{26}$$

where

$$\mathbf{h}_2(\mathbf{x}_2)=[h_{2i}]\in R^m$$

with $h_{2i}=\rho_{i0}+B_r$.

The EKF equations to estimate $\mathbf{x}_2$ are similar to (14)–(20). Note that the measurement matrix becomes $\mathbf{H}_2(k)=[H_{2ij}]\big|_{\mathbf{x}_2=\mathbf{x}_2^-(k)}\in R^{m\times(4+l)}$ with

$$H_{2i1}=\frac{1}{\rho_{i0}}\left[x-X_i+(f_1(x,\mathbf{p_c})-Y_i)\frac{\partial f_1(x,\mathbf{p_c})}{\partial x}+(f_2(x,\mathbf{p_c})-Z_i)\frac{\partial f_2(x,\mathbf{p_c})}{\partial x}\right]$$
$$H_{2i2}=1,\quad H_{2i3}=0,\quad H_{2i4}=0$$
$$H_{2ij}=\frac{1}{\rho_{i0}}\left[(f_1(x,\mathbf{p_c})-Y_i)\frac{\partial f_1(x,\mathbf{p_c})}{\partial p_{j-4}}+(f_x(x,\mathbf{p_c})-Z_i)\frac{\partial f_2(x,\mathbf{p_c})}{\partial p_{j-4}}\right],\quad j=5,6,\ldots,4+l.$$

In the Appendix, detailed algorithms are given for three common road models: straight lines, arcs, and polynomials.

In the EKF process, the nonlinear system is relinearized about each new estimate as it becomes available. Thus, the EKF is designed to work well as long as the estimates are near their true values. Therefore, the initial states of the augmented system cannot be given arbitrarily. They must not deviate from their true values too much. Fortunately, since the detailed digital map of the city is available, the curve model for each piece of road can be determined prior to the navigation process. Hence, the parameters of the curve model for the road can be regarded as the initial estimates of the parameters of the curve modeling the vehicle's path.

V. Positioning at Intersections Using IMM Algorithm

In real urban environments, the road segments are connected by intersections. Therefore, it is of great importance for the vehicle to "know" which road it is following when crossing road intersections, and then be able to use the correct road model for state-augmented EKF. In this paper, the IMM method is adopted to fulfill this task.

The IMM method is a powerful approach for adaptive estimation. In this approach, a set of models is defined to represent the possible system behavior patterns, and the overall estimate is obtained by a certain combination of the estimates from the filters

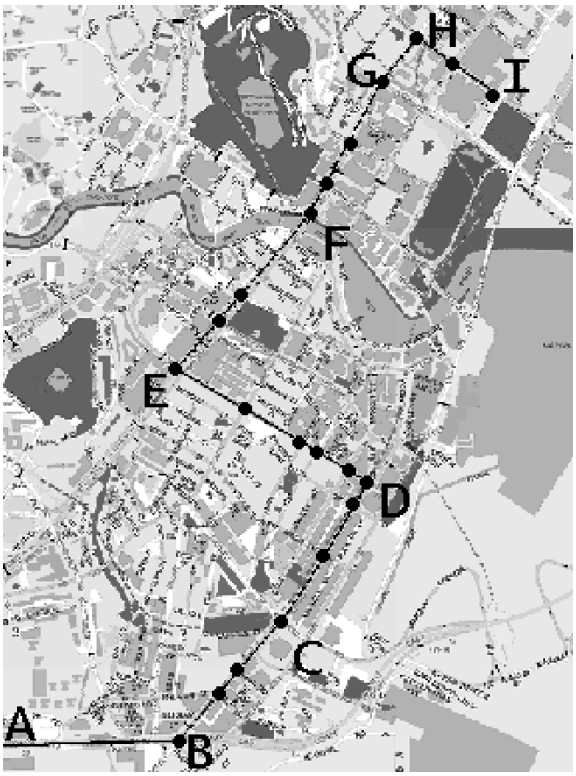

Fig. 1. Roads segmentation and intersection representation.

running in parallel, based on the individual models that match the system modes [20]. For detailed derivation of the IMM estimator, refer to [17] and [22].

A. Map Representation

The map of the environment is represented by a set of roads which are connected by a set of intersections. Fig. 1 shows an example of the road segmentation and intersection representation based on a city map, where AB, BC, …, HI denotes eight roads; along each road, the intersections are denoted by black dots. Though the segmentation of roads can be, theoretically, arbitrary, it should be neither too detailed nor too sketchy in practice. Too few roads will lead to large modeling errors. Increasing the number of roads may improve the modeling accuracy, but it will increase the burden of data storage and processing. A tradeoff needs to be made in road segmentation depending on the desired accuracy. In this paper, the roads are segmented intuitively based on the city map.

For each segmented road, M_i, $i = 1, 2, \ldots, n_r$, with n_r being the total number of roads, the following pieces of information need to be stored.

- Shape of the road, such as straight, arc, or second-order polynomial, etc. The shape of a road determines the number of parameters of the road model.
- Parameters of the road model.
- Indexes of intersections in this road.

For each intersection, I_j, $j = 1, 2, \ldots, n_i$, with n_i being the total number of intersections, the following pieces of information need to be stored.

- Position of the intersection.
- Indexes of roads that connect to this intersection.

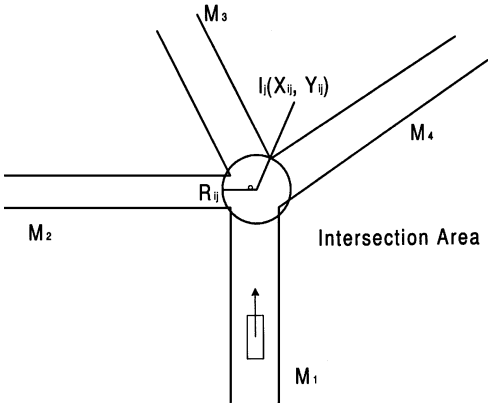

Fig. 2. Vehicle comes to an intersection.

- Radius of the intersection area R_{ij}. The intersection area is defined as a circular area which covers the intersection. As soon as the vehicle enters an intersection, the IMM method is supposed to be triggered to estimate the position of the vehicle and select the correct road model.

B. IMM Algorithm

As the vehicle enters an intersection area, the IMM algorithm will be triggered to estimate the position of the vehicle and determine the correct road that the vehicle is following. For example, as shown in Fig. 2, the vehicle moves toward intersection I_j with an circular intersection area centered at (X_{ij}, Y_{ij}) with radius R_{ij}, which connects to four roads, namely, M_1, M_2, M_3, and M_4. Generally, it is assumed that there are n_{rj} roads connected to intersection I_j, and these roads are denoted by M_l, $l = 1, 2, \ldots, n_{rj}$. As long as the vehicle enters the intersection area, i.e., the distance between the position estimates of the vehicle and the center of the intersection is less than the radius of the intersection area, the IMM method is triggered.

In this method, n_{rj} EKFs are running in parallel, each based on one road model connected to I_j. As will be seen in the rest of this section, the state estimates of each EKF will interact with each other in the IMM algorithm. Therefore, in the IMM algorithm, all the EKFs are designed without state augmentation, because the state-augmented EKFs are road-model dependent and their state estimates cannot be combined or mixed. The likelihood of each road will be calculated based on the estimates of these EKFs and will be used as the criterion of determining the correct road model.

For road model $M = M_l$, $l = 1, 2, \ldots, n_{rj}$, the continuous state-space model of the vehicle is given by (22), and can be rewritten as

$$\dot{\mathbf{x}}_{\mathrm{IMM}l} = \mathbf{F}_1 \mathbf{x}_{\mathrm{IMM}l} + \mathbf{w}_1, \qquad l = 1, 2, \ldots, n_{rj} \tag{27}$$

where $\mathbf{x}_{\mathrm{IMM}l}$ denotes the state using road model M_l. The measurement equation for road model $M = M_l$, $l = 1, 2, \ldots, n_{rj}$ is similar to (23), i.e.,

$$\boldsymbol{\rho} = \mathbf{h}_l(\mathbf{x}_{\mathrm{IMM}l}) + \mathbf{v}, \qquad l = 1, 2, \ldots, n_{rj}. \tag{28}$$

The corresponding discrete-time models of the vehicle can be written as

$$\mathbf{x}_{\mathrm{IMM}l}(k+1) = \boldsymbol{\Phi}_1 \mathbf{x}_{\mathrm{IMM}l}(k) + \mathbf{w}_{dl} \tag{29}$$

$$\boldsymbol{\rho}(k) = \mathbf{h}_j[\mathbf{x}_{\mathrm{IMM}l}(k)]. \tag{30}$$

The purpose of using the IMM method herein is to estimate the probability of each road connected to the intersection. The model of the road with the maximum probability will be considered as the road which the vehicle follows. Some probabilities needs to be defined. First, the probability of road model M_l being correct at time k is defined as the conditional probability

$$\mu_l(k) \triangleq P\{M(k) = M_l | \mathbf{Z}(k)\} \tag{31}$$

where $\mathbf{Z}(k) = \{\boldsymbol{\rho}(0), \boldsymbol{\rho}(1), \ldots, \boldsymbol{\rho}(k)\}$ is the set of measurements collected till time k. The probability of road model M_l being correct at time k, conditioned on that model M_i being correct at time $k-1$, is called model transition probability, and is defined as

$$\mu_{il} \triangleq P\{M(k) = M_l | M(k-1) = M_i\}. \tag{32}$$

In this paper, the following assumptions are made for implementing the IMM method.

Assumption 2: When the vehicle enters an intersection I_j, the road which the vehicle comes from is denoted as M_1, and other roads are labeled as $M_2, \ldots, M_{n_{rj}}$.

Assumption 3: It is assumed that the vehicle may transit from M_1 to all the road models, including itself, with equal probability.

Assumption 4: It is assumed that once the vehicle transitions from M_1 to another road M_l, the transition probability from M_l to each of the other roads will be equal and be very small.

Based on the above assumptions, the transition probability matrix for intersection I_j can be defined as

$$\begin{aligned}\mathbf{\Pi} &= \begin{bmatrix} \pi_{11} & \pi_{12} & \cdots & \pi_{1n_{rj}} \\ \pi_{21} & \pi_{22} & \cdots & \pi_{2n_{rj}} \\ \cdots & \cdots & \cdots & \cdots \\ \pi_{n_{rj}1} & \pi_{n_{rj}2} & \cdots & \pi_{n_{rj}n_{rj}} \end{bmatrix} \\ &= \begin{bmatrix} \dfrac{1}{n_r} & \dfrac{1}{n_r} & \cdots & \dfrac{1}{n_r} \\ \dfrac{1-\eta}{n_r-1} & \eta & \cdots & \dfrac{1-\eta}{n_r-1} \\ \cdots & \cdots & \cdots & \cdots \\ \dfrac{1-\eta}{n_r-1} & \dfrac{1-\eta}{n_r-1} & \cdots & \eta \end{bmatrix}\end{aligned} \tag{33}$$

where η is a positive scalar denoting the probability that the vehicle keeps following the road once it enters the road. In this paper, η is set to be 0.8.

The other two probabilities which will be used in the IMM algorithm are the predicted model probability μ_l^-, and the mixing probability $\mu_{i|l}$ given by

$$\mu_l^- \triangleq P\{M(k) = M_l | \mathbf{Z}(k-1)\} \tag{34}$$

$$\mu_{i|l} \triangleq P\{M(k-1) = M_i | M(k) = l, \mathbf{Z}(k-1)\}. \tag{35}$$

The IMM algorithm is given below [18].

Step 1: *Initialization*.

Assume that the vehicle comes from road M_1 and enters the intersection I_j at time k. For the lth EKF, $l = 1, 2, \ldots, n_{rj}$, the state for each road model $\hat{\mathbf{x}}_{\mathrm{IMM}l}(k)$ is initialized as the first four states of $\hat{\mathbf{x}}_2(k-1)$, and the covariance for each road $\mathbf{P}_{\mathrm{IMM}}j \in R^{4\times 4}$, $j = 1, 2, \ldots, n_r$ is initialized as the upper left 4×4 subarray of $\mathbf{P}_2$, where n_{rj} is the number of roads connected to this intersection, and $\hat{\mathbf{x}}_2(k-1)$ and $\mathbf{P}_2$ are the state estimate and covariance of the state-augmented EKF by using road model M_1. The initial road model probabilities are set by

$$\begin{aligned}\mu_1(k-1) &= 1 \\ \mu_k(k-1) &= 0, \qquad l = 2, \ldots, n_{rj}\end{aligned}$$

because it is certain that the vehicle comes from road M_1.

Step 2: *Interaction*.

The predicted road probability is given by

$$\mu_l^- = \sum_{i=1}^{n_{rj}} \mu_i(k-1)\pi_{il}. \tag{36}$$

The mixing probability is given by

$$\mu_{i|j} = \mu_i(k-1)\pi_{ij}/\mu_j^-. \tag{37}$$

The mixed state estimate and covariance are given by

$$\begin{aligned}\hat{\mathbf{x}}_{\mathrm{IMM0}l} &\triangleq E\{\mathbf{x}_{\mathrm{IMM}}(k-1) | M(k) = M_l, \mathbf{Z}(k-1)\} \\ &= \sum_{i=1}^{n_{rj}} \hat{\mathbf{x}}_{\mathrm{IMM}i}(k-1)\mu_{i|l}\end{aligned} \tag{38}$$

$$\begin{aligned}P_{0l}(k-1) &\triangleq \mathrm{Cov}\{\mathbf{x}_{\mathrm{IMM}}(k-1) | M(k) = M_l, \mathbf{Z}(k-1)\} \\ &= \sum_{i=1}^{n_{rj}} \Big(\mu_i(k-1) + [\hat{\mathbf{x}}_{\mathrm{IMM}i}(k-1) \\ &\quad - \hat{\mathbf{x}}_{\mathrm{IMM0}l}(k-1)] \\ &\quad = [\hat{\mathbf{x}}_{\mathrm{IMM}i}(k-1) - \hat{\mathbf{x}}_{\mathrm{IMM0}l}(k-1)]^T\Big)\mu_{i|l}.\end{aligned} \tag{39}$$

Step 3: *Prediction*.

The state and covariance are propagated as

$$\hat{\mathbf{x}}_{\mathrm{IMM}l}^-(k) = \mathbf{\Phi}_1 \hat{\mathbf{x}}_{\mathrm{IMM0}l}(k-1) \tag{40}$$

$$\mathbf{P}_{\mathrm{IMM}l}^-(k) = \mathbf{\Phi}_1 P_{0l}(k-1)\mathbf{\Phi}_1^T + \mathbf{Q}_{d1}. \tag{41}$$

Step 4: *Update*.

The measurement residual and residual covariance can be written as

$$\boldsymbol{\nu}_l(k) = \boldsymbol{\rho}(k) - \mathbf{h}_l(\hat{\mathbf{x}}_{\mathrm{IMM}l}^-(k)) \tag{42}$$

$$\mathbf{S}_l(k) = \mathbf{R} + \mathbf{H}_l \mathbf{P}_{\mathrm{IMM}l}^-(k)\mathbf{H}_l^T \tag{43}$$

where $\mathbf{H}_l$ is the corresponding Jacobian matrix. The state and covariance for each road model is updated by

$$\hat{\mathbf{x}}_{\mathrm{IMM}l}(k) = \hat{\mathbf{x}}_{\mathrm{IMM}l}^-(k) + \mathbf{K}_l \boldsymbol{\nu}(k) \tag{44}$$

$$\mathbf{P}_{\mathrm{IMM}l}(k) = \mathbf{P}_{\mathrm{IMM}l}^-(k) - \mathbf{K}_l \mathbf{S}_l(k)\mathbf{K}_l^T \tag{45}$$

where $\mathbf{K}_l$ is the filter gain for each road model

$$\mathbf{K}_l = \mathbf{P}_{\mathrm{IMM}l}^-(k)\mathbf{H}_l^T[\mathbf{S}_l(k)]^{-1}. \tag{46}$$

The likelihood function of road model M_l is given by

$$\begin{aligned}\Lambda_l(k) &\triangleq P\{\boldsymbol{\rho}(k) | \mathbf{Z}(k-1), M(k) = M_l\} \\ &= |(2\pi)^4 \mathbf{S}_j(k)|^{-(1/2)} \exp\left\{-\tfrac{1}{2}\alpha_l(k)\right\}\end{aligned} \tag{47}$$

where $\alpha_l(k)$ is the normalized innovation squared

$$\alpha_l(k) = \boldsymbol{\nu}_l(k)^T[\mathbf{S}_l(k)]^{-1}\boldsymbol{\nu}_l(k). \tag{48}$$

Step 5: *Combination and Model Probability Update*.

The probability of each road model is updated by [17]

$$\mu_l(k) \approx \mu_l^- \Lambda_l(k). \tag{49}$$

The state and covariance update are realized by the following equations:

$$\hat{\mathbf{x}}_{\mathrm{IMM}}(k) = \sum_{i=1}^{n_{rj}} \hat{\mathbf{x}}_{\mathrm{IMM}i}(k)\mu_i(k) \tag{50}$$

$$\mathbf{P}_{\mathrm{IMM}}(k) = \sum_{i=1}^{n_{rj}} \Big(\mathbf{P}_{\mathrm{IMM}i}(k) + [\hat{\mathbf{x}}_{\mathrm{IMM}i}(k) - \hat{\mathbf{x}}_{\mathrm{IMM}}(k)] \cdot [\hat{\mathbf{x}}_{\mathrm{IMM}i}(k) - \hat{\mathbf{x}}_{\mathrm{IMM}}(k)]^T\Big)\mu_i(k). \tag{51}$$

The position of the vehicle is updated as follows. Define the estimated position of the vehicle for each road model as

$$\mathbf{p}_l(k) = [\mathbf{x}_{\mathrm{IMM}l}(1) \quad y_l \quad z_l]^T, \qquad l = 1, 2, \ldots, n_{rj} \tag{52}$$

where $y_{\mathrm{IMM}l} = f_{l1}(\mathbf{x}_{\mathrm{IMM}l}(1))$ and $z_{\mathrm{IMM}l} = f_{l2}(\mathbf{x}_{\mathrm{IMM}l}(1))$. The combined position estimate is given as

$$\mathbf{p}(k) = \sum_{l=1}^{n_{rj}} \mathbf{p}_l(k)\mu_l(k). \tag{53}$$

Step 6: *Termination Detection.*

The IMM method will be terminated if the correct path has been selected after the vehicle passes the intersection. Otherwise, repeat Step 2-Step 6 if either of the following two conditions are not satisfied:

1) the vehicle has moved out of the intersection;

2) the maximum road probability

$$\max\{\mu_l(k), l = 1, 2, \ldots, n_{rj}\} > \xi \tag{54}$$

where ξ is a positive scalar near to but less than 1. In this paper, $\xi = 0.95$.

Once the IMM algorithm is terminated, the state-augmented EKF using the selected road model is reinitialized and retriggered using the road model selected by the IMM algorithm.

VI. Performance Analysis

In this section, the performance of the proposed constrained solution for solving the urban canyon environment is analyzed. The objective is to find the relationship between the pseudorange measurement errors and the user position and clock bias errors. Since in the filtering solution and the joint parameter and state estimation method, EKF is adopted to estimate the states and it is difficult to analyze its performance due to the intrinsic nonlinearity and relinearization, we shall not analyze the performance of the filtering solutions. Instead, the performance analysis is focused on point-wise solutions.

Assume that there are m GPS satellites available, with $m \geq 2$. Then, the linearized error equation is given by

$$\delta\boldsymbol{\rho} = \mathbf{H}\delta\mathbf{x} + \mathbf{v}. \tag{55}$$

Denote $\delta\boldsymbol{\rho}^*$ as the pseudorange deviation without any corruption of noises, i.e., $\delta\boldsymbol{\rho}^* = \mathbf{H}\delta\mathbf{x}$. Therefore, the noisy estimate of the position can be written as

$$\delta\hat{\mathbf{x}} = \mathbf{H}^{-1}(\delta\boldsymbol{\rho}^* + \mathbf{v}). \tag{56}$$

Since the noise $\mathbf{v}$ is zero mean, the expectation value of $\delta\hat{\mathbf{x}}$ is $\delta\mathbf{x}$.

To calculate the variance of the estimated position and receiver clock bias, let each individual pseudorange measurement have an error covariance denoted by σ and the cross correlation of errors between satellites be zero. With these assumptions, the covariance matrix $E[\mathbf{v}\mathbf{v}^T]$ for the pseudorange measurements becomes a scaled identity matrix $\sigma^2\mathbf{I}$. Hence, the covariance matrix of $\hat{\mathbf{x}}$ based on a single set of simultaneous pseudorange measurements can be written as

$$\begin{aligned}\mathbf{P} &= \mathrm{Cov}(\mathbf{x}) = \mathrm{Cov}(\delta\hat{\mathbf{x}}) \\ &= E\left[(\mathbf{H}^{-1}\mathbf{v})(\mathbf{H}^{-1}\mathbf{v})^T\right] = \left(\mathbf{H}^T\mathbf{H}\right)^{-1}\sigma^2.\end{aligned} \tag{57}$$

Define

$$\mathbf{V} = \left(\mathbf{H}^T\mathbf{H}\right)^{-1}. \tag{58}$$

By taking inverse of $(\mathbf{H}^T\mathbf{H})$, $\mathbf{V}$ can be written as

$$\mathbf{V} = \frac{\begin{bmatrix} m & -\sum_{i=1}^{m} H_i \\ -\sum_{i=1}^{m} H_i & -\sum_{i=1}^{m} H_i^2 \end{bmatrix}}{m\sum_{i=1}^{m} H_i^2 - \left(\sum_{i=1}^{m} H_i\right)^2}. \tag{59}$$

Exploring the denominator, we have

$$m\sum_{i=1}^{m} H_i^2 - \left(\sum_{i=1}^{m} H_i\right)^2 = \tfrac{1}{2}\sum_{i=1}^{m}\sum_{j=1}^{m}(H_i - H_j)^2. \tag{60}$$

Then $\mathbf{V}$ can also be written as

$$\mathbf{V} = \frac{\begin{bmatrix} m & -\sum_{i=1}^{m} H_i \\ -\sum_{i=1}^{m} H_i & \sum_{i=1}^{m} H_i^2 \end{bmatrix}}{\tfrac{1}{2}\sum_{i=1}^{m}\sum_{j=1}^{m}(H_i - H_j)^2}. \tag{61}$$

The variances of the positioning error in x direction $\delta\hat{x}$ and the receiver clock bias $\hat{B}_r$ is then estimated by

$$\sigma_x^2 = V_{11}\sigma^2 \tag{62}$$

$$\sigma_{B_r}^2 = V_{22}\sigma^2 \tag{63}$$

where

$$V_{11} = \frac{m}{\tfrac{1}{2}\sum_{i=1}^{m}\sum_{j=1}^{m}(H_i - H_j)^2}\,\sigma^2$$

$$V_{22} = \frac{\sum_{i=1}^{m} H_i^2}{\tfrac{1}{2}\sum_{i=1}^{m}\sum_{j=1}^{m}(H_i - H_j)^2}\,\sigma^2.$$

One can prove that V_{11} is a nonincreasing function with respect to m. This means that the more satellites in view are used, the better the positioning performance.

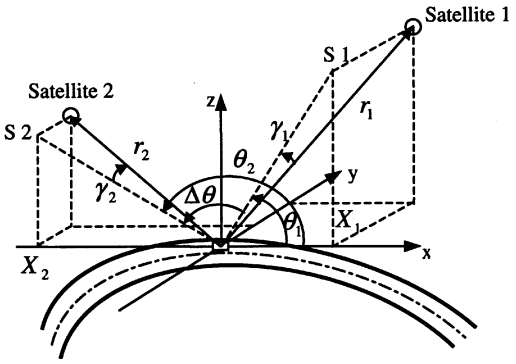

Fig. 3. GPS receiver and satellites in the body frame.

According to (5) and (6), the variance of $\hat{y}$ and $\hat{z}$ are approximately given by

$$\sigma_y^2 = (f_1'(x))^2\sigma_x^2 = (f_1'(x))^2 V_{11}\sigma^2 \tag{64}$$

$$\sigma_z^2 = (f_2'(x))^2\sigma_x^2 = (f_2'(x))^2 V_{11}\sigma^2. \tag{65}$$

It is clear that the positioning performance depends on the sum of the magnitudes of $H_i - H_j, 1 \le i, j \le m$, and $i \ne j$. It is valuable to examine the relationship between the satellite-road geometry and the magnitude of $H_i - H_j$, $1 \le i, j \le m$ and $i \ne j$. In the following part of this section, the relationship is analyzed for the case $m = 2$.

Obviously, as $m = 2$, the positioning performance depends on the magnitude of $(H_1 - H_2)$ only, i.e., the larger the magnitude, the better the performance. For simplicity of analysis, the following analysis is with respect to the body frame, which is defined to be a right-handed coordinate frame fixed at the vehicle with the origin at the center of the vehicle, the x axis pointing forward, the y axis pointing left, and the z axis pointing upward. Since distances remain unchanged under rectangular coordinate transformation, the proposed approach is applicable to any rectangular coordinate systems. It is obvious that in the body frame, the coordinates of the vehicle is (0, 0, 0) and $f_1'(x) = dz/dx = 0$. Therefore, the following equalities hold:

$$H_1 - H_2 = \frac{X_2}{r_2} - \frac{X_1}{r_1} \tag{66}$$

where r_1 and r_2 are user-to-satellite distances as shown in Fig. 3. Denote the angles between the user-to-satellite vectors and the $x - z$ plane as γ_1 and γ_2, respectively, and denote the angles between the projections of the user-to-satellite vectors onto the $x - z$ plane and the x axis as θ_1 and θ_2, respectively. Then, we have

$$\begin{aligned} H_1 - H_2 &= \frac{r_2\cos(\gamma_2)\cos(\theta_2)}{r_2} - \frac{r_1\cos(\gamma_1)\cos(\theta_1)}{r_1} \\ &= \cos(\gamma_2)\cos(\theta_1 + \Delta\theta) - \cos(\gamma_1)\cos(\theta_1). \end{aligned} \tag{67}$$

Since the vehicle travels in an urban environment, γ_1 and γ are very small, which means $\cos(\gamma_1), \cos(\gamma_2) \approx 1$. Therefore

$$H_1 - H_2 = \cos(\theta_1 + \Delta\theta) - \cos(\theta_1). \tag{68}$$

Since $0 \le \theta_1 + (\Delta\theta/2) < \pi$ and $0 \le \Delta\theta/2 < \pi$, we have $H_1 - H_2 < 0$, and $(\partial(H_1 - H_2))/\partial\Delta\theta = -\sin(\theta_1 + \Delta\theta) \le 0$, which means that $H_1 - H_2$ is a nonpositive decreasing function. This means that the larger the $\Delta\theta$, the smaller the $H_1 - H_2$, or, the larger the magnitude of $H_1 - H_2$. In other words, the larger the angle between the projections of the two user-satellites vectors on the $x - z$ plane, the better the positioning performance. Therefore, in the applications, when there are more than two satellites in view, we may use all the satellite information to compute the position of the receiver, or we may choose the two satellites with the maximal angle between the two user-to-satellite vectors.

According to (64) and (65), $\sigma_y^2 = \sigma_z^2 = 0$, and the distance root mean square error (DRMS) is

$$\mathrm{DRMS} = \sigma_x = \frac{\sqrt{2}}{|H_1 - H_2|}\sigma. \tag{69}$$

The position dilution of precision (PDOP) is defined as

$$\mathrm{PDOP} = \mathrm{DRMS}/\sigma = \frac{\sqrt{2}}{|H_1 - H_2|}. \tag{70}$$

Note that PDOP is related not only to the user-to-satellite geometry, but also to the direction of the path of the vehicle. In the common GPS positioning mode with enough satellites, the PDOP is inversely proportional to the volume of a body which is formed by the intersection points of the user-satellite vectors with the unit sphere centered at the user, and the GPS performance can be predicted by only evaluating the volume. Similarly, in the case of only two available satellites, the GPS performance indicator PDOP can be predicted by only evaluating the angle between the two user-to-satellite vectors. The larger the angle, the better the GPS performance.

VII. Simulation Studies

In this section, the effectiveness of the proposed method is demonstrated through computer simulations. Assume that the vehicle equipped with a GPS receiver travels somewhere with the local horizontal plane coordinate system originated at latitude $\lambda = 1°23' 15.9''$, longitude $\phi = 103°56'32.5''$, and height $h = 0$ m in the earth-centered–earth-fixed (ECEF) coordinate frame. The road map of the navigation environment with respect to the local horizontal plane frame is shown in Fig. 1, where the grey polygons represent buildings in this area. When generating the available GPS satellite signals, it is assumed that the heights of these buildings range from 60–180 m. The vehicle is assumed to travel from point A along the labeled path to point I.

To compare the performances of the proposed approach and the conventional EKF method which utilizes the system model (12) and (13) all the time for GPS positioning in urban canyon environments, simulations are performed using both methods under the same conditions. Fig. 4(a) and (b) show the positioning errors using the conventional EKF method without path modeling and the proposed approach with path modeling, respectively. Fig. 4(c) shows the corresponding number of available GPS satellite signals. Obviously, as the number of available GPS satellites becomes less than four, the positioning distance error by using conventional EKF without path modeling increases fast. By contrast, the positioning distance errors are much lower for the case of using the proposed method with path modeling. In fact, the mean distance error by using the conventional method is 1205 m, while the mean distance error by using the proposed method is only 0.436 m. In Fig. 4(b),

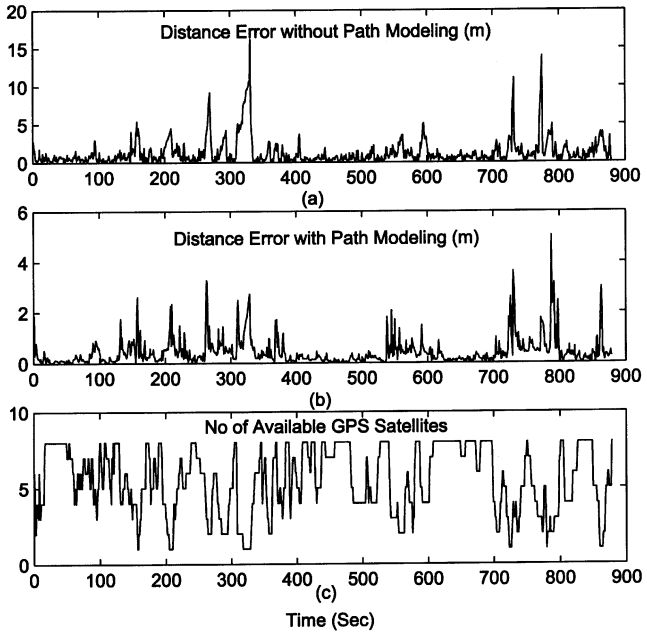

Fig. 4. Simulation results.

there are several impulses in the distance errors. These pulses appear when the vehicle just enters an intersection where the IMM method is reinitialized, and the position estimates are obtained using the IMM method by combining the state estimates from all the extended Kalman filtering running in parallel. As shown in Fig. 4(b), the distance errors at these time instants may drop fast as more signals are received.

From Fig. 4(b), it can be easily seen that the positioning distance errors are much lower in the case that the number of available GPS satellites is larger. When the number of available GPS satellites is one, the positioning distance error using the proposed method may also increase. For example, during the period $t \in [318, 329]$ s, the number of available GPS satellites is one. The distance errors during this period increase from 0.564 m to 2.73 m. This is one limitation of the proposed method. Nevertheless, the divergence of distance errors using the proposed method is much slower than that using the conventional EKF method without path modeling, and fortunately, the period of only one available GPS satellite is short in usual urban environments and the distance errors are within acceptable levels, therefore, the path modeling method can be regarded as a successful method to solve the urban canyon problem.

It is also found that the IMM method can work effectively. As the vehicle moves and more data are collected, the probability of the correct road increases while the probabilities of the wrong roads decrease. In fact, the terminating conditions 1) and 2) with high ξ can guarantee that before the IMM algorithm is terminated, the road model can be correctly determined.

VIII. Conclusion

In this paper, a constrained method has been presented by approximately modeling the path of the vehicle in the urban canyon environment as pieces of straight lines. By adding this constraint to the set of pseudorange equations, the minimum number of available satellites reduces to two, which is satisfied in many urban canyon environments. In this paper, point-wise solutions and filtering solutions are developed systematically. In addition, a state augmentation method is also presented to estimate the parameters of the straight line and the positioning information simultaneously. Based on the augmented system, EKF is employed to estimate the states. When the vehicle enters intersection area, based on the models of all the roads connected to this intersection, the IMM method is used to simultaneously estimate the position of the vehicle and determine the road which the vehicle follows. Simulation results show the feasibility and effectiveness of the proposed approach.

Appendix

Notice that most roads in urban area can be modeled by straight lines, helix, and lower-order polynomials. Therefore, the algorithms for these three types of roads are discussed in detail herein. For more winding roads, they can be modeled by higher-order polynomials and the algorithms can be similarly achieved according to the analysis in Section IV.

A. Straight Roads

Define a straight road as

$$\begin{cases} y = p_{10}x + p_{20} \\ z = p_{30}x + p_{40} \end{cases} \tag{71}$$

where p_{10}, p_{20}, p_{30}, and p_{40} are four known parameters. Without losing generality, assume that this straight line models the center line of the road. As the vehicle travels along this road, its path may not coincide with the center line of the road. Hence, we shall assume that its path is still a straight line with the same form but slightly different parameters, i.e.,

$$\begin{cases} y = p_1x + p_2 \\ z = p_3x + p_4 \end{cases} \tag{72}$$

where p_1, p_2, p_3, and p_4 are four unknown parameters to be estimated. The algorithm for joint parameter and state estimation follows the analysis in Section IV, where the augmented state is given by

$$\mathbf{x}_2 = [\,x \quad B_r \quad \dot{x} \quad \dot{B}_r \quad p_1 \quad p_2 \quad p_3 \quad p_4\,]^T. \tag{73}$$

The EKF algorithm follows (14)–(20), with

$$\mathbf{H}_2(k) = \left.\frac{\partial \mathbf{h}_2(\mathbf{x}_2)}{\partial \mathbf{x}_2}\right|_{\mathbf{x}_2=\mathbf{x}_2^-(k)} = [H_{2ij}]|_{\mathbf{x}_2=\mathbf{x}_2^-(k)} \in R^{m\times 8}$$

where

$$H_{2i1} = \frac{1}{\rho_{i0}}\,[x - X_i + p_1(p_1x + p_2 - Y_i) + p_3(p_3x + p_4 - Z_i)]$$
$$H_{2i2} = 1, \quad H_{2i3} = 0, \quad H_{2i4} = 0$$
$$H_{2i5} = \frac{1}{\rho_{i0}}\,[x(p_1x + p_2 - Y_i)], \quad H_{2i6} = \frac{1}{\rho_{i0}}\,(p_1x + p_2 - Y_i)$$
$$H_{2i7} = \frac{1}{\rho_{i0}}\,[x(p_3x + p_4 - Z_i)], \quad H_{2i8} = \frac{1}{\rho_{i0}}\,(p_3x + p_4 - Z_i).$$

B. Arc Roads

Some winding roads can be modeled by arcs. Assume that all the navigation computations are implemented with respect to a local navigation frame (north–east–down). Often, the arc road

does not lie on the horizontal plane. Instead, it is an ascending or descending arc. Assume that the road ascends/descends linearly, then, a common model for ascending/descending arc roads is given by

$$\begin{cases} x = p_{10} + p_{30}\cos(p_{40}z + p_{50}) \\ y = p_{20} + p_{30}\sin(p_{40}z + p_{50}) \end{cases} \tag{74}$$

where p_{10}–p_{50} are five known parameters. Similarly, the path of the vehicle along this road can be modeled by

$$\begin{cases} x = p_1 + p_3\cos(p_4 z + p_5) \\ y = p_2 + p_3\sin(p_4 z + p_5) \end{cases} \tag{75}$$

where p_1–p_5 are five unknown parameters to be estimated. The corresponding augmented state is given by

$$\mathbf{x}_2 = [\,z \quad B_r \quad \dot{z} \quad \dot{B}_r \quad p_1 \quad p_2 \quad p_3 \quad p_4 \quad p_5\,]^T \tag{76}$$

and the algorithm for joint parameter and state estimation follows the analysis in Section IV, where

$$\mathbf{H}_2(k) = \left.\frac{\partial \mathbf{h}_2(\mathbf{x}_2)}{\partial \mathbf{x}_2}\right|_{\mathbf{x}_2 = \mathbf{x}_2^-(k)} = [H_{2ij}]\big|_{\mathbf{x}_2 = \mathbf{x}_2^-(k)} \in R^{m\times 9}$$

with

$$\begin{aligned}
H_{2i1} &= \frac{1}{\rho_{i0}}\{-[p_1 + p_3\cos(p_4 z + p_5) - X_i] \\
&\quad \cdot p_3 p_4 \sin(p_4 z + p_5) + [p_2 + p_3\cos(p_4 z + p_5) - Y_i] \\
&\quad \cdot p_3 p_4 \cos(p_4 z + p_5) + (z - Z_1)\} \\
H_{2i2} &= 1, \quad H_{2i3} = 0, \quad H_{2i4} = 0 \\
H_{2i5} &= \frac{1}{\rho_{i0}}[p_1 + p_3\cos(p_4 z + p_5) - X_i] \\
H_{2i6} &= \frac{1}{\rho_{i0}}[p_2 + p_3\cos(p_4 z + p_5) - Y_i] \\
H_{2i7} &= \frac{1}{\rho_{i0}}\{[p_1 + p_3\cos(p_4 z + p_5) - X_i]\cos(p_4 z + p_5) \\
&\quad + [p_2 + p_3\cos(p_4 z + p_5) - Y_i]\sin(p_4 z + p_5)\} \\
H_{2i8} &= \frac{1}{\rho_{i0}}\{-[p_1 + p_3\cos(p_4 z + p_5) - X_i]p_3 z\sin(p_4 z + p_5) \\
&\quad + [p_2 + p_3\cos(p_4 z + p_5) - Y_i]p_3 z\cos(p_4 z + p_5)\} \\
H_{2i9} &= \frac{1}{\rho_{i0}}\{-[p_1 + p_3\cos(p_4 z + p_5) - X_i]p_3\sin(p_4 z + p_5) \\
&\quad + [p_2 + p_3\cos(p_4 z + p_5) - Y_i]p_3\cos(p_4 z + p_5)\}.
\end{aligned}$$

The parameters of the road model p_{10}–p_{50} can be regarded as the initial estimates of the parameters, p_1–p_5, of the arc model of the vehicle's path.

C. Roads Modeled by Polynomials

Most roads can be modeled by polynomials. In this subsection, we shall take the third-order polynomial as an example. Assume that road is modeled by

$$\begin{cases} x = p_{10}y^3 + p_{20}y^2 + p_{30}y + p_{40} \\ z = p_{50}y^3 + p_{60}y^2 + p_{70}y + p_{80} \end{cases} \tag{77}$$

where p_{10}–p_{80} are five known parameters. Similarly, the path of the vehicle along this road can be modeled by

$$\begin{cases} x = p_1 y^3 + p_2 y^2 + p_3 y + p_4 \\ z = p_5 y^3 + p_6 y^2 + p_7 y + p_8 \end{cases} \tag{78}$$

where p_1–p_8 are eight parameters to be estimated. The corresponding state is given by

$$\mathbf{x}_2 = [\,z \quad B_r \quad \dot{z} \quad \dot{B}_r \quad p_1 \quad \cdots \quad p_8\,]^T \tag{79}$$

and the matrix $\mathbf{H}_2$ is given by

$$\mathbf{H}_2(k) = \left.\frac{\partial \mathbf{h}_2(\mathbf{x}_2)}{\partial \mathbf{x}_2}\right|_{\mathbf{x}_2 = \mathbf{x}_2^-(k)} = [H_{2ij}]\big|_{\mathbf{x}_2 = \mathbf{x}_2^-(k)} \in R^{m\times 12}$$

with

$$\begin{aligned}
H_{2i1} &= \frac{1}{\rho_{i0}}\{-(p_1 y^3 + p_2 y^2 + p_3 y + p^4 - X_i) \\
&\quad \cdot (3p_1 y^2 + 2p_2 y + p_3) + (y - Y_i) + (p_5 y^3 + p_6 y^2 \\
&\quad + p_7 y + p^8 - Z_i)(3p_5 y^2 + 2p_6 y + p_7)\} \\
H_{2i2} &= 1, \quad H_{2i3} = 0, \quad H_{2i4} = 0 \\
H_{2i5} &= \frac{1}{\rho_{i0}}(p_1 y^3 + p_2 y^2 + p_3 y + p^4 - X_i)y^3 \\
H_{2i6} &= \frac{1}{\rho_{i0}}(p_1 y^3 + p_2 y^2 + p_3 y + p^4 - X_i)y^2 \\
H_{2i7} &= \frac{1}{\rho_{i0}}(p_1 y^3 + p_2 y^2 + p_3 y + p^4 - X_i)y \\
H_{2i8} &= \frac{1}{\rho_{i0}}(p_1 y^3 + p_2 y^2 + p_3 y + p^4 - X_i) \\
H_{2i9} &= \frac{1}{\rho_{i0}}(p_5 y^3 + p_6 y^2 + p_7 y + p^8 - Z_i)y^3 \\
H_{2i10} &= \frac{1}{\rho_{i0}}(p_5 y^3 + p_6 y^2 + p_7 y + p^8 - Z_i)y^2 \\
H_{2i11} &= \frac{1}{\rho_{i0}}(p_5 y^3 + p_6 y^2 + p_7 y + p^8 - Z_i)y \\
H_{2i12} &= \frac{1}{\rho_{i0}}(p_5 y^3 + p_6 y^2 + p_7 y + p^8 - Z_i).
\end{aligned}$$

REFERENCES

[1] J. A. Farrell and M. Barth, *The Global Positioning System and Inertial Navigation*. New York: McGraw-Hill, 1999.

[2] S. S. Ge, T. Goh, T. Y. Jiang, R. Koopman, S. W. Chan, and A. M. Fong, "Terrestrial navigation based on integrated GPS and INS," in *Proc. SPIE Conf. Enhanced and Synthetic Vision*, vol. 3364, Orlando, FL, Apr. 13–17, 1998, pp. 348–358.

[3] M. Tsakiri, A. Kealy, and M. Stewart, "Urban canyon vehicle navigation with integrated GPS/GLONASS/DR systems," *Navigation: J. Inst. Navigation*, vol. 46, no. 3, pp. 161–174, 1999.

[4] N. El-Sheimy and K. P. Schwarz, "Navigating urban areas by VISAT—A mobile mapping system integrating GPS/INS/digital cameras for GIS applications," *Navigation: J. Inst. Navigation*, vol. 45, no. 4, pp. 275–285, 1998.

[5] J. D. Weiss and F. Shields, "GPS/INS integration in a severe urban environment," in *Proc. IEEE Position Location, Navigation Symp.*, 1998, pp. 432–440.

[6] C. Vlcek, P. Mclain, and M. Murphy, "GPS/dead reckoning for vehicle tracking in the 'urban canyon' environment," in *Proc. IEEE–IEE Vehicle and Information Systems Conf.*, Ottawa, ON, Canada, 1993, pp. A34–A41.

[7] M. Phatak and M. Chansarkar, "Position fix from three GPS satellites and altitude: A direct method," *IEEE Trans. Aerosp. Electron. Syst.*, vol. 35, pp. 350–354, Jan. 1999.

[8] M. A. Sturza, "GPS navigation using three satellites and a precise clock," in *Global Positioning System—Papers Published in Navigation*. Alexandria, VA: Inst. Navigation, 1984, vol. 2.

[9] D. Walsh, S. Capaccio, D. Lowe, P. Daly, P. Shardlow, and G. Johnston, "Real time differential GPS and GLONASS vehicle positioning in urban areas," in *Proc. IEEE Conf. Intelligent Transportation Systems*, 1997, pp. 514–519.

[10] J. M. McLellan and J. P. Battie, "Testing and analysis of OEM GPS sensor boards for AVL applications," in *Proc. IEEE Position Location, Navigation Symp.*, 1994, pp. 512–519.
[11] M. Rothblatt, "Urban area performance of GPS receiver with simultrac capability," *IEEE Aerosp. Electron. Syst. Mag.*, pp. 29–33, Aug. 1992.
[12] J. M. Mendel, *Lessons in Estimation Theory for Signal Processing, Communications, and Control*. Englewood Cliffs, NJ: Prentice-Hall, 1995.
[13] I. J. Cox, "A review of statistical data association techniques for motion correspondence," *Int. J. Comput. Vis.*, vol. 10, no. 1, pp. 53–66, 1993.
[14] R. Simmons and S. Koenig, "Probabilistic robot navigation in partially observable environment," in *Proc. Int. Joint Conf. Artificial Intelligence (IJCAI)*, 1995, pp. 1080–1087.
[15] A. R. Cassandra, L. P. Kaelbling, and J. A. Kurien, "Acting under uncertainty: Discrete Bayesian models for mobile-robot navigation," in *Proc. IEEE/RSJ Int. Conf. Intelligent Robots and Systems (IROS)*, 1996, pp. 963–972.
[16] D. Fox, W. Burgard, F. Dellaert, and S. Thrun, "Monte Carlo localization: Efficient position estimation for mobile robots," in *Proc. Nat. Conf. Artificial Intelligence (AAAI)*, 1999, pp. 343–349.
[17] J. B. Kim, Y. K. Lee, and C. W. Lee, "On the applications of the interacting multiple model algorithm for enhancing noisy speech," *IEEE Trans. Speech Audio Processing*, vol. 8, no. 3, pp. 349–352, 2000.
[18] M. Yeddanapudi and Y. Bar-Shalom, "IMM estimation for multitarget–multisensor air traffic surveillance," *Proc. IEEE*, vol. 85, pp. 80–94, Jan. 1997.
[19] X. R. Li and Y. Bar-Shalom, "Performance prediction of the interacting multiple model algorithm," *IEEE Trans. Aerosp. Electron. Syst.*, vol. 29, pp. 755–771, July 1993.
[20] ——, "Multiple-model estimation with variable structure," *IEEE Trans. Automat. Contr.*, vol. 41, pp. 478–493, Apr. 1996.
[21] H. A. P. Blom and Y. Bar-Shalom, "The interacting multiple model algorithm for systems with Markovian switching coefficients," *IEEE Trans. Automat. Contr.*, vol. 33, pp. 780–783, Aug. 1988.
[22] Y. Bar-Shalom, *Estimation and Tracking: Principles, Techniques and Software*. Norwood, MA: Artech House, 1993.
[23] J. Guivant, E. Nebot, and S. Baiker, "Localization and map building using laser range sensors in outdoor applications," *J. Robot. Syst.*, vol. 17, no. 10, pp. 565–583, 2000.
[24] H. H. S. Liu and G. K. H. Pang, "Accelerometer for mobile robot positioning," *IEEE Trans. Ind. Applicat.*, vol. 37, pp. 812–819, May/June 2001.
[25] A. E. Gamble and P. N. Jenkins, "Low cost guidance for the multiple launch rocket system (MLRS) artillery rocket," *IEEE Aerosp. Electron. Syst. Mag.*, vol. 16, pp. 33–39, Jan. 2001.
[26] J. K. Ray, M. E. Cannon, and P. Fenton, "GPS code and carrier multipath mitigation using a multiantenna system," *IEEE Trans. Aerosp. Electron. Syst.*, vol. 37, pp. 183–195, Jan. 2001.
[27] C. W. Jang, J. C. Juang, and F. C. Kung, "Adaptive fault detection in real-time GPS positioning," *Proc. Inst. Elect. Eng.—Radar, Sonar, Navigation*, vol. 147, no. 5, pp. 254–258, 2000.

Youjing Cui received the B.E. and M.E. degrees from Northwestern Polytechnical University, Xi'an, China, in 1995 and 1997, respectively.

During 1998–2001, she was a Research Scholar working toward the Ph.D. degree in the Department of Electrical and Computer Engineering, National University of Singapore, Singapore. In 2002, she joined Singapore Technologies Dynamics Pte Ltd., Singapore. Her current research interests are in the fields of mobile robots, path planning, navigation, and sensor fusion.

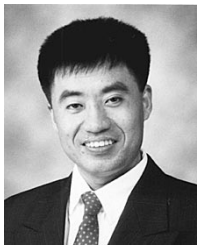

Shuzhi Sam Ge (S'90–M'92–SM'00) received the B.Sc. degree from Beijing University of Aeronautics and Astronautics (BUAA), Beijing, China, in 1986, and the Ph.D. degree and the Diploma of Imperial College (DIC) from the Imperial College of Science, Technology and Medicine, University of London, London. U.K., in 1993.

He has been with the Department of Electrical and Computer Engineering, National University of Singapore, Singapore, since 1993, and is currently as an Associate Professor. He visited Laboratoire de'Automatique de Grenoble, Grenoble, France in 1996, the University of Melbourne, Melbourne, Australia in 1998, 1999, and the University of Petroleum, Shanghai Jiaotong University, Shanghai, China, in 2001. He has authored and coauthored over 100 international journal and conference papers, two monographs, and coinvented two patents. His current research interests are control of nonlinear systems, neural networks and fuzzy logic, robot control, real-time implementation, path planning, and sensor fusion.

Dr. Ge served as an Associate Editor on the Conference Editorial Board of the IEEE Control Systems Society in 1998 and 1999, has been serving as an Associate Editor, IEEE TRANSACTIONS ON CONTROL SYSTEMS TECHNOLOGY since 1999, and as a Member of the Technical Committee on Intelligent Control of the IEEE Control System Society since 2000. He was the recipient of the 1999 National Technology Award, the 2001 University Young Research Award, and the 2002 Temasek Young Investigator Award, Singapore.